The AAPS Journal, Vol. 19, No. 4, July 2017 (© 2017)
DOI: 10.1208/s12248-017-0073-9

Research Article

Theme: Recent Advances in Musculoskeletal Tissue Engineering
Guest Editor: Aliasger K. Salem

Controlled Release of Vanadium from a Composite Scaffold Stimulates Mesenchymal Stem Cell Osteochondrogenesis

S. D. Schussler,[1] K. Uske,[2] P. Marwah,[2] F. W. Kemp,[3] J. D. Bogden,[3] S. S. Lin,[4] and Treena Livingston Arinzeh[2,5]

Received 6 December 2016; accepted 6 March 2017; published online 22 March 2017

Abstract. Large bone defects often require the use of autograft, allograft, or synthetic bone graft augmentation; however, these treatments can result in delayed osseous integration. A tissue engineering strategy would be the use of a scaffold that could promote the normal fracture healing process of endochondral ossification, where an intermediate cartilage phase is later transformed to bone. This study investigated vanadyl acetylacetonate (VAC), an insulin mimetic, combined with a fibrous composite scaffold, consisting of polycaprolactone with nanoparticles of hydroxyapatite and beta-tricalcium phosphate, as a potential bone tissue engineering scaffold. The differentiation of human mesenchymal stem cells (MSCs) was evaluated on 0.05 and 0.025 wt% VAC containing composite scaffolds (VAC composites) *in vitro* using three different induction media: osteogenic (OS), chondrogenic (CCM), and chondrogenic/osteogenic (C/O) media, which mimics endochondral ossification. The controlled release of VAC was achieved over 28 days for the VAC composites, where approximately 30% of the VAC was released over this period. MSCs cultured on the VAC composites in C/O media had increased alkaline phosphatase activity, osteocalcin production, and collagen synthesis over the composite scaffold without VAC. In addition, gene expressions for chondrogenesis (Sox9) and hypertrophic markers (VEGF, MMP-13, and collagen X) were the highest on VAC composites. Almost a 1000-fold increase in VEGF gene expression and VEGF formation, as indicated by immunostaining, was achieved for cells cultured on VAC composites in C/O media, suggesting VAC will promote angiogenesis *in vivo*. These results demonstrate the potential of VAC composite scaffolds in supporting endochondral ossification as a bone tissue engineering strategy.

KEY WORDS: biocomposite; bone; insulin mimetic; mesenchymal stem cells; vanadium.

INTRODUCTION

An estimated 6.5 million fractures are treated in the USA per year. Although bone has a regenerative capacity, approximately 10 to 20% of fractures fail to heal properly due to nonunion and delayed healing (1). Autografts and allografts are commonly used to treat these bone defects (2). However, limitations are associated with their use, such as tissue morbidity in the case of autografts and the potential for disease transmission and lack of biological activity in the case of allografts. Underlying medical conditions, such as osteoporosis and diabetes, can also have an impact on the healing duration and outcome. Therefore, alternative strategies are being sought to promote bone repair.

In tissue engineering/regenerative medicine, scaffolds or biomaterials are being designed to deliver growth factors, cells, or other osteogenic inducers and be osteoconductive and provide suitable mechanical support to promote bone tissue formation (3–5). Bioceramics, such as hydroxyapatite (HA), β-tricalcium phosphate (β-TCP), and biphasic calcium phosphate (BCP) (a combination of HA and β-TCP), have demonstrated bone bioactivity, *i.e.*, bond to bone tissue, proven biocompatibility, and excellent osteoconductivity, making them a potential candidate for bone tissue engineering applications (6). However, due to

[1] Department of Chemical, Biological and Pharmaceutical Engineering, New Jersey Institute of Technology, Newark, New Jersey 07102, USA.
[2] Department of Biomedical Engineering, New Jersey Institute of Technology, University Heights, Newark, New Jersey 07102, USA.
[3] Department of Preventive Medicine and Community Health, New Jersey Medical School, Rutgers University, Newark, New Jersey 07103, USA.
[4] Department of Orthopaedic Surgery, New Jersey Medical School, Rutgers University, Newark, New Jersey 07103, USA.
[5] To whom correspondence should be addressed. (e-mail: arinzeh@njit.edu)

bioceramics' brittle mechanical properties, their use has been restricted to specific applications (2). Therefore, bioceramics have been incorporated with various types of natural or synthetic polymers to create highly porous biocomposite materials with improved mechanical properties (7–10). Bioceramics are also known to interact with growth factors, proteins, and cells, thus making biocomposites suitable for bone tissue engineering applications (3,11–15).

Growth factors such as BMP-2 and BMP-7 have been used in clinical applications for bone repair (10,13), but drawbacks exist, such as the supraphysiological dose, adverse reactions, poor shelf life, and sensitivity to sterilization techniques (10). Using a small molecule growth factor mimetic may be a solution for some of the aforementioned drawbacks. For example, vanadium and the organic vanadium salts, such as vanadyl acetylacetonate (VAC), are known insulin mimetics (16–19) and have been shown to increase callus cartilage, vascularity, bone formation, and mechanical properties while reducing the healing time of small bone fractures in preclinical studies (20,21). Insulin and insulin-like growth factor (IGF) are evolutionarily conserved hormones that regulate growth, metabolism, bone resorption, and development (22–24). Abnormalities in insulin production such as type 1 diabetes mellitus can lead to reduced bone mineral density, early-onset osteopenia, osteoporosis, and increased risk of fractures (22,23). The use of insulin or insulin-like mimetics can accelerate the bone healing process in diabetic and nondiabetic animal models by promoting endochondral ossification (23,25) where cartilage is later transformed to bone. However, uncontrolled insulin delivery can lead to hypoglycemia (26–31). Using VAC as insulin mimetic may circumvent this issue (20,21). Vanadium is a potent inhibitor of protein tyrosine phosphatases (PTPases) (16,32,33). Vanadium mimics the action of insulin by inhibiting PTPase, resulting in increased levels of activated insulin receptor-β subunits (16,27,32,34,35). Osteoblasts express insulin receptors and respond to exogenous insulin by increasing collagen synthesis, osteocalcin, and alkaline phosphatase production (23,24,36). Insulin signaling in osteoblasts also has been shown to be a positive regulator of postnatal bone acquisition and bone resorption.

In this study, we incorporated VAC into a bioceramic composite scaffold and evaluated the osteogenic differentiation of human mesenchymal stem cells (MSCs) on the scaffold *in vitro*. We examined MSC differentiation using three different induction media: osteogenic, chondrogenic, and osteochondrogenic, *i.e.*, a combination of chondrogenic induction followed by osteogenic induction to mimic the endochondral ossification process during fracture healing *in vivo*. Inducing endochondral ossification in MSC-based approaches for bone repair may be a promising strategy leading to robust bone formation *in vivo* (37–45). The release of VAC from the composite scaffold also was characterized over time.

MATERIALS AND METHODS

Composite Scaffold Fabrication

Polycaprolactone (PCL, M_n ~ 70–90 kDa; Sigma-Aldrich, St. Louis, MO, USA) was dissolved in methylene chloride (Thermo Fisher, Walthman, MA, USA) at 17% *w/v* ratio. Ceramic nanoparticles of 30% (*w/w*) of 20/80 (*w/w*) hydroxyapatite/beta-tricalcium phosphate (HA/beta-TCP) (Berkeley Advanced Biomaterials, Berkeley, CA, USA) were added to the PCL solution. Vanadyl acetylacetonate (VAC) (Sigma-Aldrich) was dissolved in deionized (DI) water at 10 mg/mL concentration. To generate the VAC composite, 0.05 or 0.025% (*w/w*) of VAC was added to the PCL solution containing the ceramic nanoparticles. The VAC and ceramics were mixed with PCL on a magnetic stir plate for a minimum of 1 h. Prior to electrospinning, PCL/ceramic or PCL/ceramic/VAC dispersions were sonicated with a probe ultrasonicator (Sonifier® S450-D, Branson, Danbury, CT, USA) for 2 min. The PCL/ceramic or PCL/ceramic/VAC dispersions were electrospun by placing them in a syringe having a 12-gauge needle and ejecting at 7 mL/h flow rate using a syringe pump (Harvard Apparatus, Holliston, MA, USA). At the tip of the needle, a voltage of 25 to 30 kV was applied and the scaffolds were collected on an adjacent metal plate that was at 30 to 40 cm distance from the tip of the needle. Postelectrospinning, the scaffolds were left to aerate in a desiccator for 3 to 5 days.

Scaffold Characterization

Samples were examined using scanning electron microscopy (SEM, LEO 1530 Gemini, Germany). Scaffolds were sputter coated with gold-palladium. An accelerating voltage of 3–5 kV and a working distance of 5–9 mm were used for viewing and capturing images. Measurements were taken at ten random locations per sample for fiber diameter and interfiber spacing using ImageJ software (National Institute of Health, USA), according to previously reported methods (46). Four different samples per scaffold group were analyzed.

Mechanical properties were determined by tensile testing using an Instron 3342 mechanical tester (Instron Corporation, Norwood, MA, USA) following previously reported protocols (47,48). Briefly, scaffolds were cut into 7 cm by 1 cm strips. The thickness of the strips was measured in the middle and 1.5 cm from the end of each strip. Scaffolds were placed in tensile grips with a 4-cm gauge length between the grips and tested using a crosshead speed of 3 cm/min. The strips were hydrated in deionized water for 1 h at room temperature and tested wet. Stress-strain curves were recorded. The Young's moduli and maximum tensile stress were determined. Ten samples per scaffold group were tested.

Characterization of VAC Release

To evaluate the vanadium release, VAC composites were cut into 12-mm diameter disk having a thickness of 0.4 mm. Prior to the initiation of the study, the scaffolds were UV sterilized for 30 min. Scaffolds were placed in 24-well polypropylene culture dishes (Corning Corp., Corning NY, USA), submerged in 500 μL of phosphate buffered saline (PBS, Invitrogen Corp., Carlsbad, CA, USA), and incubated at 37°C. The PBS from each sample was collected and replenished with fresh PBS at predetermined time points over 28 days to coincide with time points for cell culture experiments. Samples were stored at −20°C prior to analysis. The released vanadium concentrations were then determined

using a Perkin Elmer Z5100 electrothermal heated graphite atomizer with Zeeman background correction (Perkin Elmer Corp., Norwalk, CT, USA) as previously described (21). Four samples per scaffold group per time point were analyzed.

In Vitro Cell Studies

For cell culture, composite scaffolds containing 0.05 wt% VAC (0.05 VAC composite), 0.025 wt% of VAC (0.025 VAC composite), or without VAC (composite control) were UV sterilized for 30 min, cut into 6-mm diameter disks with thicknesses of 0.3 to 0.4 mm, and placed in 96-well polypropylene culture dishes (Corning). Human MSCs were isolated from whole bone marrow aspirates (Lonza, Inc., Walkersville, MD, USA), from three male donors, 18 to 30 years old, and cultured using standard protocols (46,49). MSCs at passage 2 were seeded at approximately 18×10^4 cells/cm^2 on each scaffold and cultured at 37°C and 5% CO_2 in a humidified incubator. Schematic representation of the feeding strategy is shown in Fig. 1. Cells on the scaffolds were cultured in (1) control standard growth medium (GM) consisting of DMEM-low glucose (Invitrogen) containing 10% fetal bovine serum (Hyclone, Logan, UT, USA) and 1% antibiotic-antimycotic (Invitrogen); (2) osteogenic induction media (OS) consisting of GM supplemented with 10 mM β-glycerolphosphate (Sigma-Aldrich), 50 μM ascorbic acid (WAKO Pure Chemicals, VA, USA), and 100 nM dexamethasone (Sigma-Aldrich); (3) chondrogenic induction media (CCM) consisting of DMEM-high glucose (Invitrogen) supplemented with 1 mM sodium pyruvate (Sigma-Aldrich), 0.17 mM ascorbic acid (WAKO Pure Chemicals), 0.1 mM dexamethasone (Sigma-Aldrich) 0.35 mM L-proline (Sigma-Aldrich), 4 mM L-glutamine (Invitrogen), 1% antibiotic-antimycotic (Invitrogen), 1% ITS + premix (Becton Dickinson, Franking Lakes, NJ, USA), and 10 ng/mL TGF-β3 (ProSpecbio, New Brunswick, NJ, USA); and (4) osteochondrogenic induction media (C/O) consisting of CCM for 14 days followed by OS for up to 28 days. A sample size of four per group was used for all the assays described below. Studies were repeated per MSC donor to establish reproducibility.

Cell Growth and Biochemical Analyses

For cell growth, alkaline phosphatase activity, and osteocalcin production assays, scaffolds containing cells were washed with deionized water and cells were lysed with 0.01 wt% Triton X-100 (Sigma-Aldrich). Cell growth was evaluated using Quanti-iT PicoGreen dsDNA Assay Kit (Invitrogen) where the cell number can be correlated from the fluorescence intensity of the labeled DNA. The cell lysate was combined with the assay reagents and allowed to incubate for 5 min at room temperature. Fluorescence was measured using excitation at 485 nm and emission at 528 nm (FLX800, Biotek, Winooski, VT, USA). The cell number was determined using a standard curve of known MSC number.

Alkaline phosphatase (ALP) is an early osteogenic marker expressed by hypertrophying chondrocytes and preosteoblasts and mineralizing osteoblast (50–52). The ALP activity was determined based on the conversion of *p*-nitrophenyl phosphate to *p*-nitrophenol according to the manufacturer's protocol (Sigma-Aldrich). The cell lysate was combined with the assay buffer and allowed to incubate at 37°C for 30 min. Post-incubation, the reaction was stopped using 0.1 N NaOH. Absorbance was measured at 405 nm (Emax, Molecular Devices, Sunnyvale, CA, USA). The ALP activity was determined relative to a *p*-nitrophenol standard curve.

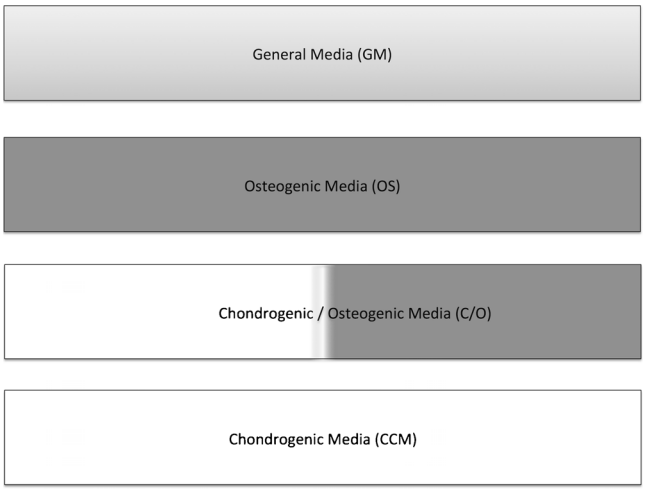

Fig. 1. Overview of *in vitro* MSC induction strategy

Osteocalcin was used as a marker for mature osteoblasts (35). Cell lysate was assayed for intact osteocalcin using an ELISA kit for human osteocalcin (Invitrogen). The assay was performed as per manufacturer's instructions. Absorbance was measured at 405 nm (Emax, Molecular Devices). The osteocalcin concentration was determined based on a calibration curve of known osteocalcin concentrations.

Hydroxyproline (HYP) was used as measure of total collagen content. Hydrolysis of the samples was performed using 12 M HCL (Sigma-Aldrich) followed by a 3-h incubation at 120°C. Post-incubation, 50 μL of individual samples was placed in a 96-well plate and left to dry overnight at 60°C. The HYP content was measured by the reaction of oxidized hydroxyproline with 4-(dimethylamino)benzaldehyde (DMAB) (Sigma-Aldrich) which results in a colorimetric change. The samples were incubated at 60°C for 90 min. Post-incubation, the absorbance was measured at 560 nm (Emax, Molecular Devices). The HYP/collagen content was determined relative to a HYP standard curve.

Sulfated glycosaminoglycan (sGAG) content was measured using a glycosaminoglycan assay (Blyscan Assay, Biocolor, UK). The sGAGs from scaffold samples were extracted using papain digestion, and the assay was performed as per manufacturer's instructions. The absorbance was measured at 656 nm (Emax, Molecular Devices), and the concentration of the sGAGs was determined relative to a chondroitin sulfate standard curve.

Cell growth and ALP activity were determined at 4, 7, 14, 21, and 28 days in culture. The osteocalcin production, GAG, and HYP content were performed at 28 days in culture. The results were normalized to the cell number for each sample and were reported as mean ± standard deviation.

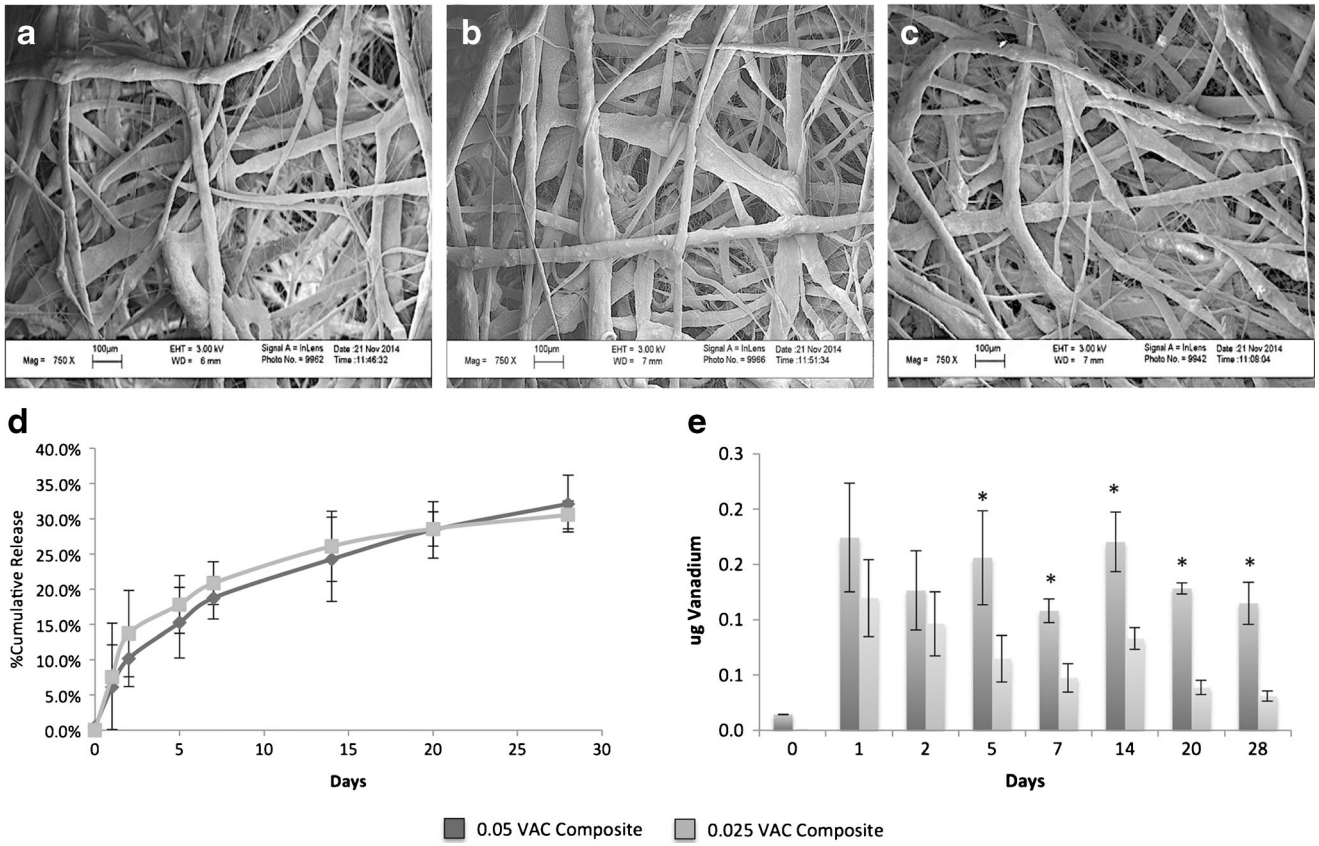

Fig. 2. SEM images: **a** 0.05 VAC composite, **b** 0.025 VAC composite, and **c** composite control. Vanadium release from composite scaffold: **d** percent cumulative release and **e** release over time (*$p < 0.05$ between 0.05 VAC composite and 0.025 VAC composite, $n = 4$ per group per time point, values are mean ± standard deviation (SD))

Cell Morphology and Immunostaining for Extracellular Matrix Deposition

Cell morphology and extracellular matrix (ECM) deposition was evaluated at 28 days by confocal microscopy. Scaffolds were fixed in 4% paraformaldehyde. The cell morphology was observed by staining for F-actin filaments of the cytoskeleton (rhodamine phalloidin, Thermo Fisher) and nucleus (DAPI, Thermo Fisher). ECM deposition on the mats was detected by staining for collagen type I using primary antibody (goat anti-collagen type 1, Millipore) and secondary antibody (rabbit anti-goat IgG, Alexa Fluor 488 phalloidin conjugate, Thermos Fisher, USA) and collagen type II using primary antibody (mouse anti-collagen type 2, EMD Millipore, Germany) and secondary antibody (donkey anti-mouse IgG Alexa Fluor 488 phalloidin conjugate, R&D Systems, USA). Vascular endothelial growth factor (VEGF) was detected by using mouse anti-VEGF Alexa Fluor 488 antibody (Abcam, UK) specific for isoform VEGF189, isoform VEGF165, and isoform VEGF121.

Gene Expression

Gene expression was evaluated for Sox9, Runx2, MMP-13, collagen type X, and VEGF-α. Sox9 is a marker of chondrogenic differentiation and is highly expressed by condensing MSCs (53–57). Runx2 is considered a master regulator of MSC differentiation along the osteogenic lineage and regulates the expression of genes necessary for bone development (46,53,57–59). MMP-13, collagen type X, and VEGF-α were used as markers to measure endochondral ossification. MMP-13 and collagen type X are expressed as chondrocyte hypertrophy (51,60–62). VEGF is an essential coordinator of chondrocyte death, extracellular matrix remodeling, angiogenesis, and new bone formation (63–65). Total RNA was isolated from the scaffolds at days 2, 7, 14, 16,

Table I. Fiber Diameter and Interfiber Spacing Measurements

Composition	Fiber diameter (μm)	Interfiber spacing (μm)
0.05 VAC composite	67.0 ± 25.1	171.4 ± 72.0
0.025 VAC composite	57.9 ± 13.8	193.5 ± 80.4
Composite control	54.2 ± 11.2	182.2 ± 90.9

Table II. Mechanical Properties of Composites

Composition	Young's modulus (MPa)	Maximum tensile stress (MPa)
0.05 VAC composite	27.1 ± 4.0	1.34 ± 0.19
0.025 VAC composite	30.1 ± 1.5	1.54 ± 0.21
Composite control	26.2 ± 4.3	1.28 ± 0.23

and 28 using RNeasy micro kit (Qiagen, Valencia, CA). Briefly, samples were immersed in lysis buffer and incubated at room temperature for 30 min followed by homogenization of the scaffolds. The RNA isolation followed the manufacturer's protocol. Quantitative RT-PCR analysis was performed with the One Step QuantiTect SYBR Green RT-PCR Kit (Qiagen, Valencia, CA) using the MX4000 detection system (Stratagene, Santa Clara, CA) according to the manufacturer's instructions. The reaction was performed as previously described in (46,47). The target gene expression was first normalized to the expression of the housekeeping gene RPLPO for the same sample (ΔCt). To show the effects of the VAC, the target gene expression for the VAC scaffolds was normalized to the control composite (ΔΔCt). The $2^{-\Delta\Delta Ct}$ method was used to convert normalized gene expression levels to fold differences (66). For RT-PCR evaluation, a sample size of three was used per group per time point.

Statistical Analysis

All assays and testing were performed with a sample size of $n = 4$ per group per time point, unless otherwise specified. Studies were performed in triplicate and per donor to establish reproducibility. Results were evaluated for normal distribution using a Shapiro-Wilk test and were analyzed using a one-way ANOVA and a *post hoc* Tukey test performed using SPSS Statistics software. Statistically significant differences were determined for $p < 0.05$.

RESULTS

Scaffold Characterization

Similar fiber morphology, fiber diameters, and interfiber spacing were observed for the scaffolds as seen in Fig. 2a–c and Table I. Average fiber diameters ranged from

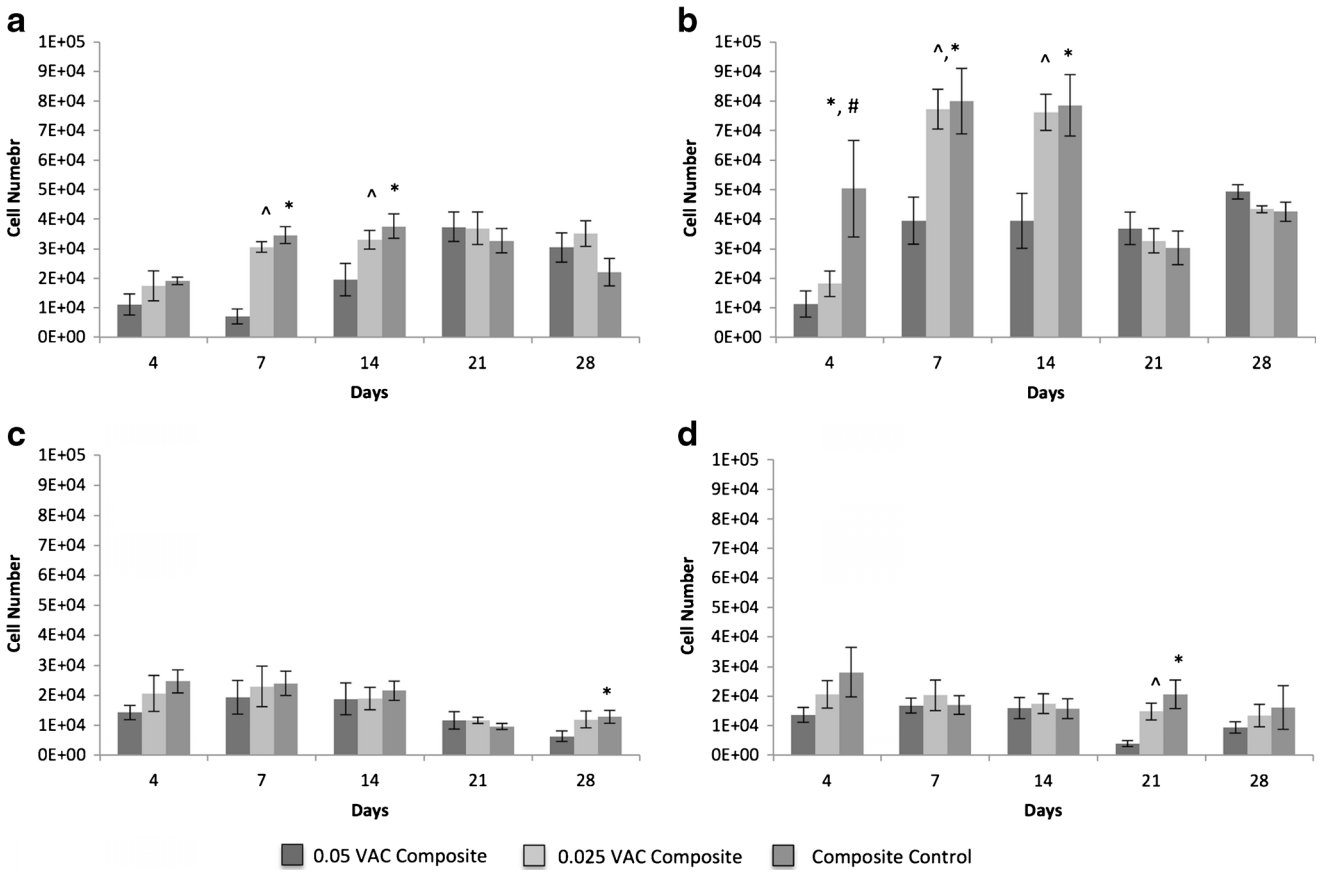

Fig. 3. Cell number on the scaffolds in **a** growth media (GM), **b** osteogenic media (OS), **c** chondrogenic media (CCM), and **d** chondrogenic/osteogenic media (C/O) (*$p < 0.05$ between composite control and 0.05 VAC composite, #$p < 0.05$ between composite control and 0.025 VAC composite, ^$p < 0.05$ between 0.025 VAC and 0.05 VAC composites, $n = 4$ per group per time point, values are mean ± SD)

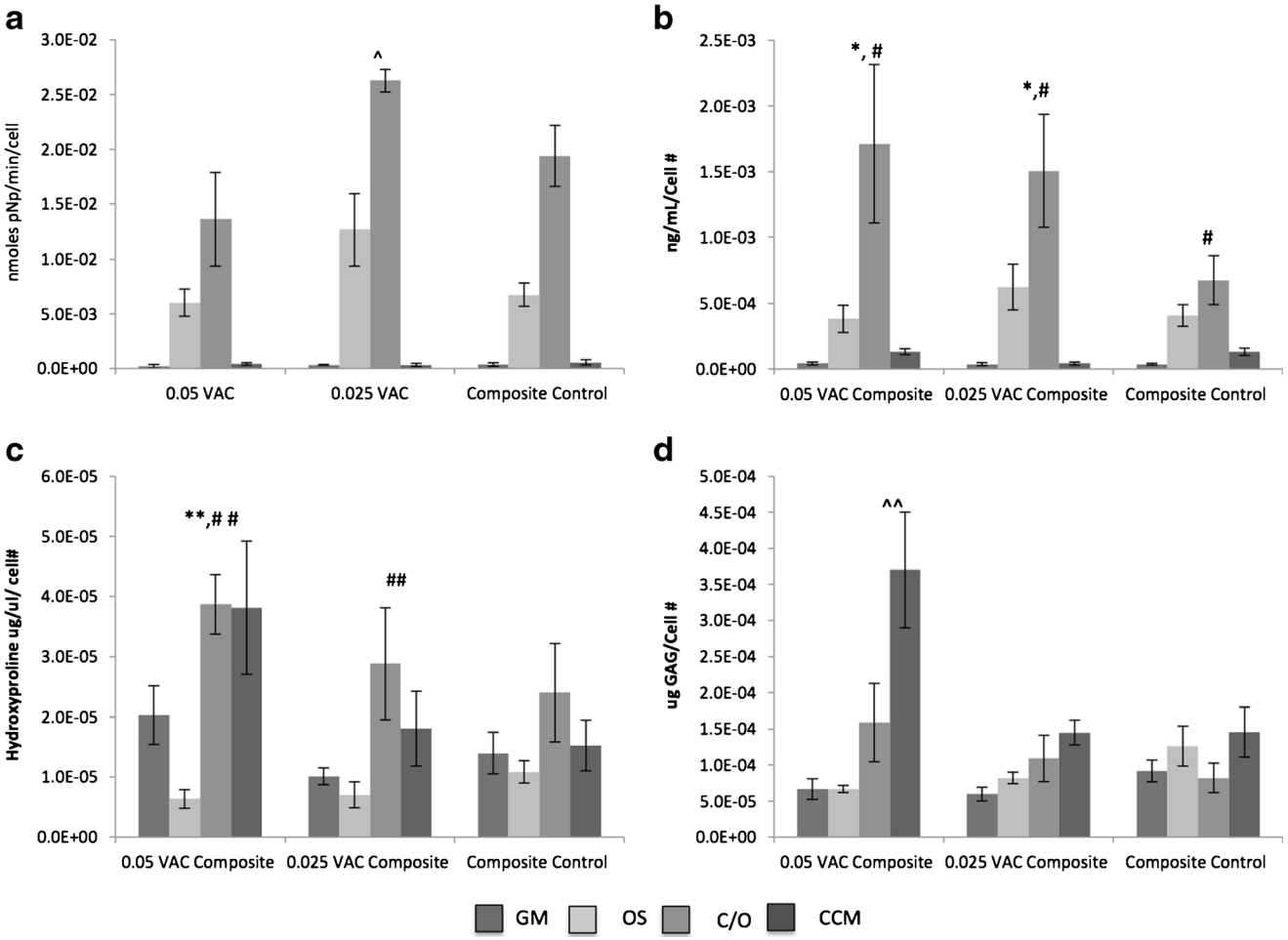

Fig. 4. **a** Alkaline phosphatase activity normalized to cell number at day 28 (^$p < 0.05$ between 0.025 VAC composite and 0.05 VAC and composite control). **b** Osteocalcin production normalized to cell number at day 28 (*$p < 0.05$ between 0.05 VAC composite and composite control in C/O media, #$p < 0.05$ between C/O media and OS media, #$p < 0.0$ between C/O and CCM media). **c** Collagen production normalized to the cell number at day 28 (**$p < 0.05$ between 0.05 VAC composite in C/O and CCM media and composite control, ##$p < 0.05$ between C/O media and osteogenic media). **d** sGAG production normalized to the cell number at day 28 (^^$p < 0.05$ between 0.05 VAC composite in CCM media and 0.025 VAC and composite control). $n = 4$ per group, values are mean ± SD

approximately 50 to 70 μm and average interfiber spacing ranged from approximately 170 to 195 μm. The VAC composites had similar moduli and maximum tensile stresses as the composite control (Table II).

Vanadium Release

The 0.05 and the 0.025 VAC composites had similar percent cumulative release (Fig. 2d) but differed in the amount released where 0.025 VAC had significantly lower VAC amounts than 0.05 VAC from days 5 through 28 (Fig. 2e). About 30% of VAC was released over the 28 days without an initial burst release.

Cell Growth

The different VAC composite scaffolds and the composite control were able to support cell growth in GM media (Fig. 3). Lower cell numbers were determined for the 0.05 VAC composites as compared to the composite control at early time points of days 4, 7, and 14 in GM and OS media and at day 21 in C/O media. By 28 days, the cell number for the VAC composites was comparable to the composite control in different media conditions.

Biochemical Analyses

MSCs cultured on the 0.025 VAC composite in the C/O media had the highest ALP activity as compared to the 0.05 VAC composite and composite control ($p < 0.05$) (Fig. 4a). MSCs cultured on 0.025 VAC composite had the highest ALP production as compared to the 0.05 VAC composite and the composite control in OS media ($p < 0.05$). The highest ALP activity for the different composites was determined for cells cultured in C/O media as compared to the OS, GM, and CCM media ($p < 0.05$). MSCs cultured on 0.05 and 0.025 VAC composites had the highest osteocalcin production in C/O media as compared to composite control ($p < 0.05$) (Fig. 4b). The highest level of osteocalcin production was observed for MSCs cultured on the different scaffolds in C/O media as compared to MSCs cultured in OS, CCM, and GM media ($p < 0.05$).

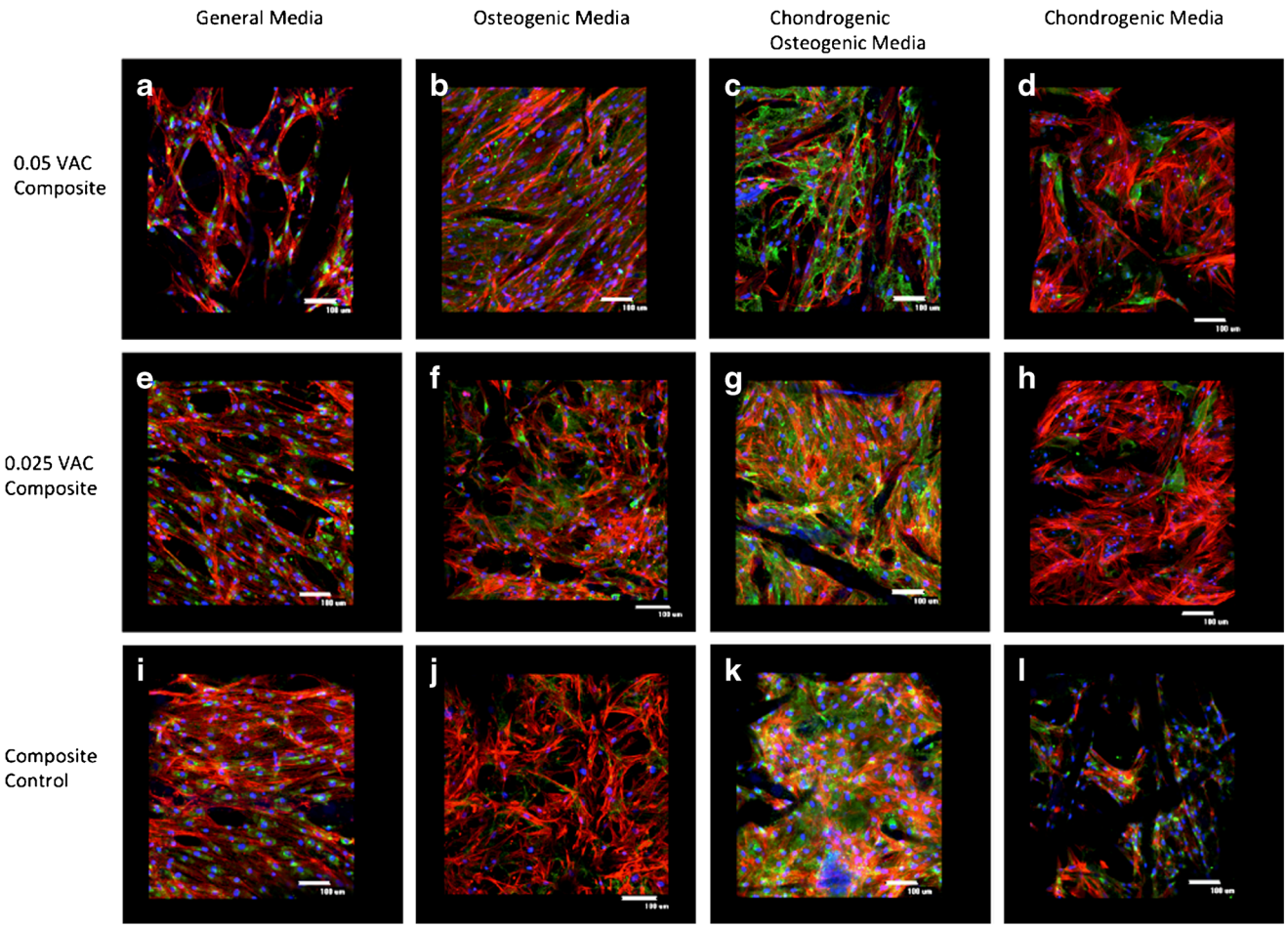

Fig. 5. Confocal microscopy images of immunostaining for collagen type I at day 28: **a–d** 0.05 VAC composite; **e–h** 0.025 VAC composite; **i–l** composite control. Cells are stained for cytoskeleton (F-actin, *red*), nucleus (DAPI, *blue*), and collagen type I (*green*)

The highest amount of collagen, as determined by HYP content, was for MSCs cultured on the 0.05 VAC composite in both C/O and CCM media ($p < 0.05$) (Fig. 4c). Collagen was highest in the C/O cultured cells as compared to OS cultured cells for all groups tested ($p < 0.05$). The highest amount of sGAG was also detected for 0.05 VAC composite in CCM media ($p < 0.05$) (Fig. 4d).

Cells cultured in C/O media appeared to have the greatest staining for collagen type I across the different scaffolds, whereas the 0.05 VAC composite group in the different media showed the greatest staining for collagen type II (Figs. 5 and 6). Collagen type II matrix production was also observed for MSCs cultured on the 0.025 VAC composite and the composite control in CCM media (Fig. 6). VEGF staining appeared to be incorporated within the extracellular matrix (Fig. 7). The greatest intensity of VEGF staining was observed for cells cultured in C/O media for the different scaffolds tested. Higher intensity was observed for the VAC composites as compared to composite control. The 0.05 and 0.025 VAC composite groups also showed VEGF staining for MSCs cultured in OS media.

Gene Expression

Gene expressions for Runx2, Sox9, MMP-13, collagen X, and VEGF at day 28 are shown in Fig. 8. Runx2 expression increased on VAC composites in GM media at early time points in comparison to composite control (data not shown) and was higher for the 0.05 VAC composite by day 28 (Fig. 8a). Sox9 expression decreased for the cells cultured on the VAC composites in comparison to composite control in OS and CCM media (Fig. 8b). For cells cultured on the VAC composites in C/O media, Sox9 decreased by day 16 (data not shown); however, by day 28, Sox9 increased (Fig. 8b). An increase in MMP-13 expression was determined for cells in C/O culture (4- and 5-fold increase in gene expression for 0.05 VAC and 0.025 VAC composites, respectively) as compared to composite control (Fig. 8c). An increase in collagen type X expression was determined for cells cultured on the 0.025 VAC composite in the C/O culture (Fig. 8d). Ten- to 1000-fold increase in VEGF expression was determined for both 0.05 and 0.025 VAC composites as compared to the composite control (Fig. 8e). The fold change was the highest for the C/O media at the 28-day time point ($p < 0.05$).

DISCUSSION

In this study, we used the electrospinning process to produce porous composites incorporated with VAC, an insulin mimetic, and demonstrated controlled release of VAC from the composite. Both low and high concentrations of VAC containing scaffolds had an overall cumulative

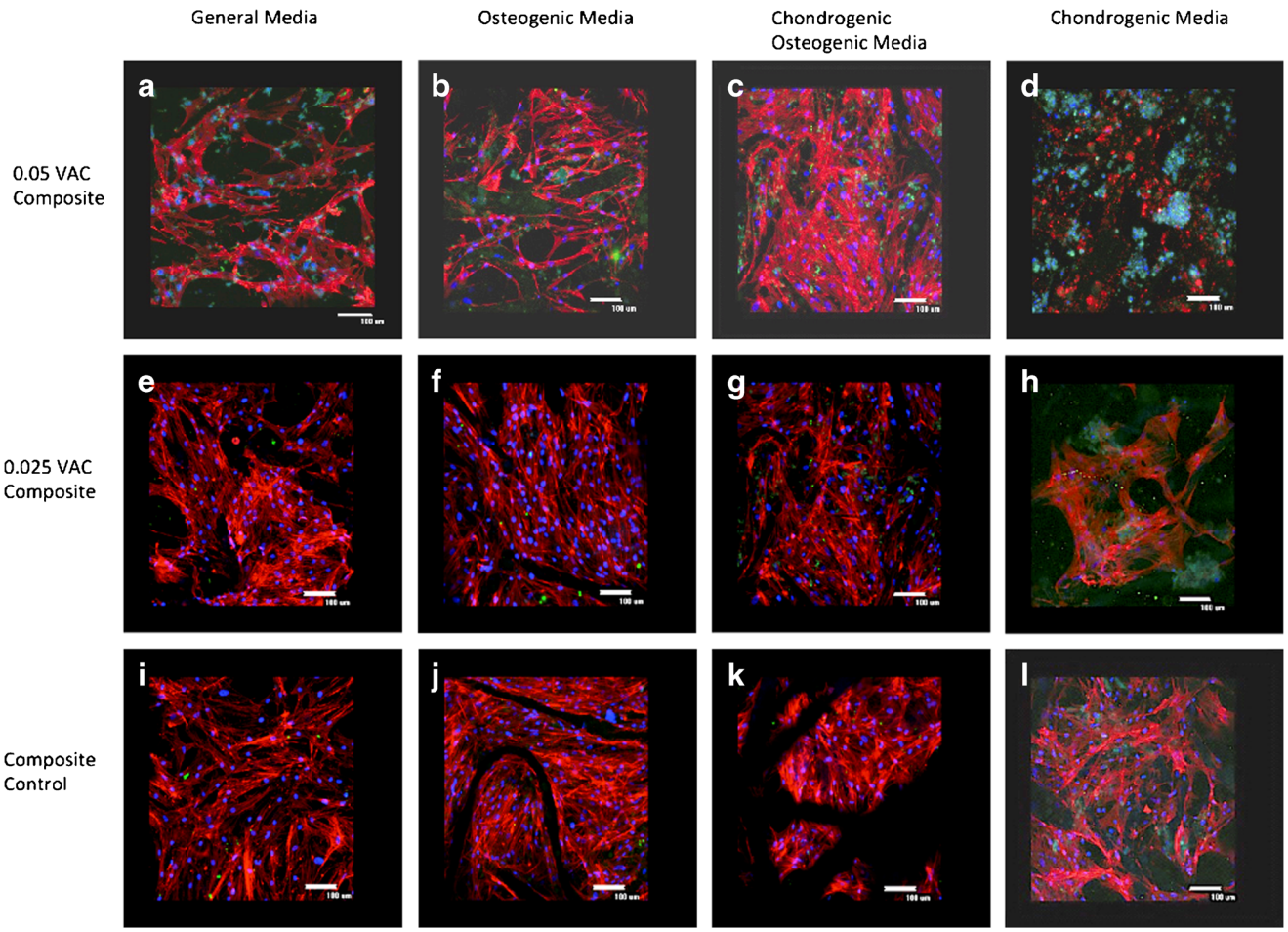

Fig. 6. Confocal microscopy images of immunostaining for collagen type II at day 28: **a–d** 0.05 VAC composite; **e–h** 0.025 VAC composite; **i–l** composite control. Cells are stained for cytoskeleton (F-actin, *red*), nucleus (DAPI, *blue*), and collagen type II (*green*)

release of 30%. The VAC composites supported cell growth and promoted MSC differentiation. Based on matrix production, the higher concentration of VAC supported greater osteochondrogenesis as compared to the lower concentration of the VAC composite and composite control. Furthermore, the osteochondrogenesis induction strategy may prove to be a good *in vitro* model for endochondral ossification.

Electrospun scaffolds can be produced with nonwoven three-dimensional fibrous structures that are favorable for cell attachment and proliferation and tissue growth (7,11,14,46,49,67). Scaffolds with highly porous structures allow for cell infiltration, vascularization, and nutrient and waste transport (68–70). Furthermore, this process creates scaffolds with a high surface area to volume ratio, making electrospun scaffolds desirable as a delivery vehicle for biomolecules such as growth factors, cells, DNA, RNA, or other small molecules (5,7,11,14,71–75). The composite scaffold in this study, having large fiber diameters and interfiber spacing, has been shown to support cell growth as well as ingrowth into the scaffold, which may be favorable for tissue ingrowth *in vivo* (46,48). By incorporating high levels of VAC, 0.05 wt%, in the composite scaffold, however, lower cell numbers were detected at early time points in growth and induction media. Studies have shown that high levels of vanadium can be toxic to cells, whereas low levels can induce cellular proliferation (76–78). By the end of the study, the cell number for the 0.05 VAC composite was comparable to the composite control, demonstrating that the higher VAC levels in this study were cytocompatible. Recent studies performed by Paglia *et al.* have demonstrated the therapeutic effect of VAC when both directly injected or released from a calcium sulfate ($CaSO_4$) carrier in a rat femur fracture site in a nondiabetic BB Wistar model (20,21). In these studies, the injected VAC was rapidly cleared from the femur fracture site (21), and the amount used could be reduced using the $CaSO_4$ carrier (20). Studies did not show an inhibitory effect on cellular proliferation (19–21). Local administration of VAC at the fracture site increased the cartilaginous callus formation, followed by increase in mineralized callus, vascularization, and increase in the callus mechanical strength (20,21). In this study, VAC was incorporated into a biocomposite that could provide long-term VAC release. Providing a sustained amount of VAC in more challenging large bone defects may be necessary to increase the osteogenic activity and promote bone healing.

The C/O induction strategy was used to mimic endochondral ossification. Recent literature and our studies indicate that this approach (endochondral ossification) to evaluate *in vitro* bone formation is more representative of bone formation and healing (39,40,43,45). This strategy induced higher levels of bone biochemical markers, such as ALP, osteocalcin, and collagen type I matrix formation for all

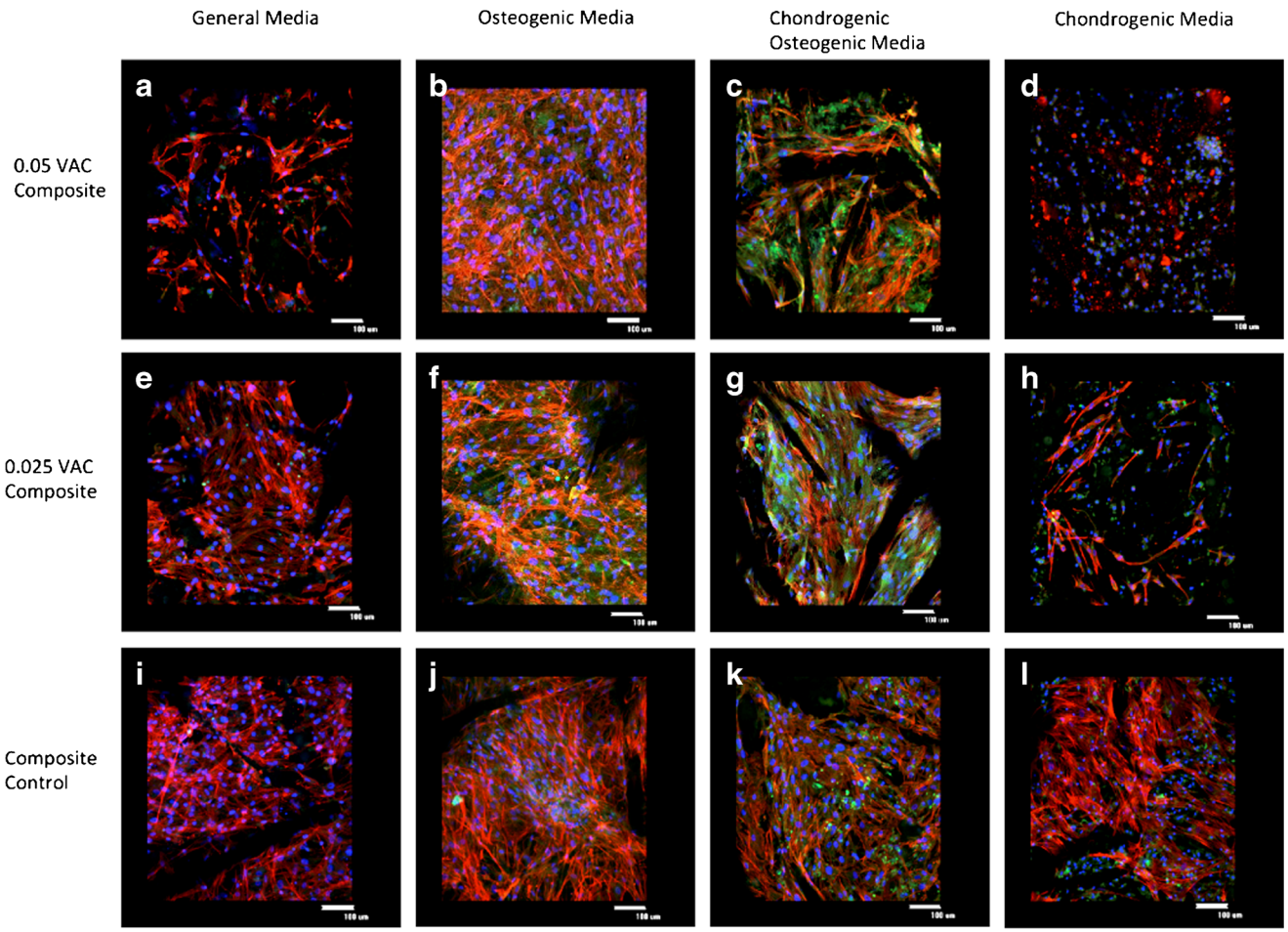

Fig. 7. Confocal microscopy images of immunostaining for VEGF at day 28: **a–d** 0.05 VAC composite; **e–h** 0.025 VAC composite; **i–l** composite control. Cells are stained for cytoskeleton (F-actin, *red*), nucleus (DAPI, *blue*), and VEGF (*green*)

of the composites tested as compared to osteogenic media. Vanadium salts can induce collagen type I production (17,18,76,79) while inhibiting ALP production (17,80). In our work, the inhibition of ALP was not observed. ALP is produced by hypertrophic chondrocytes, preosteoblast, and osteoblasts (52,81,82) and plays a crucial role in the matrix mineralization and calcification process (33,83). At day 28, cells cultured in C/O media overall showed the highest ALP activity for the media tested, and the 0.025 VAC composite had the highest expression as compared to the other composites. Osteocalcin is one of the noncollagenous proteins in the bone extracellular matrix (35). It is secreted by osteoblasts (35) and hypertrophic chondrocytes (84) and plays a critical role during the bone resorption process. It is used as a marker of bone formation. The highest osteocalcin production was observed for cell cultured in C/O media and for the VAC composites in C/O media. Recent findings demonstrate that chondrocytes can convert into osteoblasts (41). As hypertrophy is induced, certain subpopulations of chondrocytes may turn into osteoblasts thus increasing osteocalcin production (41). Matrix formation is an important factor for successful scaffold integration to the host tissue. As described, studies have shown that the use of vanadium compounds both *in vitro* and *in vivo* induces collagen production (16,18–21,26). The 0.05 VAC composite was able to stimulate higher levels of collagen production for cells cultured in C/O and CCM media than the other composites. In addition, cells cultured in C/O media had more collagen production than in OS media although collagen type I immunostaining was observed in the GM media. These studies used male donors; the gender differences need to be further studied to evaluate if donor gender will have an effect in the results (85,86).

During endochondral bone formation as chondrocytes proliferate, they create a cartilaginous extracellular matrix. Sulfated GAGs are major components of the cartilage extracellular matrix and are indicators of chondrogenesis and cartilage formation (25). Cells cultured on the 0.05 VAC composite in CCM media showed the highest level of sGAG formation as compared to the other composites. Sox9 is expressed by chondrocytes of the proliferating and prehypertrophic zones (87). Cells on VAC composites had an increase in Sox9 gene expression in GM, CCM, and C/O. The levels of Sox9 expression reduced over time in GM and CCM media and remained upregulated in C/O media for the duration of the study indicating prehypertrophic conditions. Studies show that Sox9 can be a negative regulator of cartilage vascularization, inhibiting the terminal differentiation of hypertrophic chondrocytes by suppressing VEGF expression (87). Even though Sox9 was upregulated in the C/O media conditions, it did not affect VEGF, MMP-13, and collagen type X expression, which are hypertrophic markers. VEGF gene expression was the highest on VAC

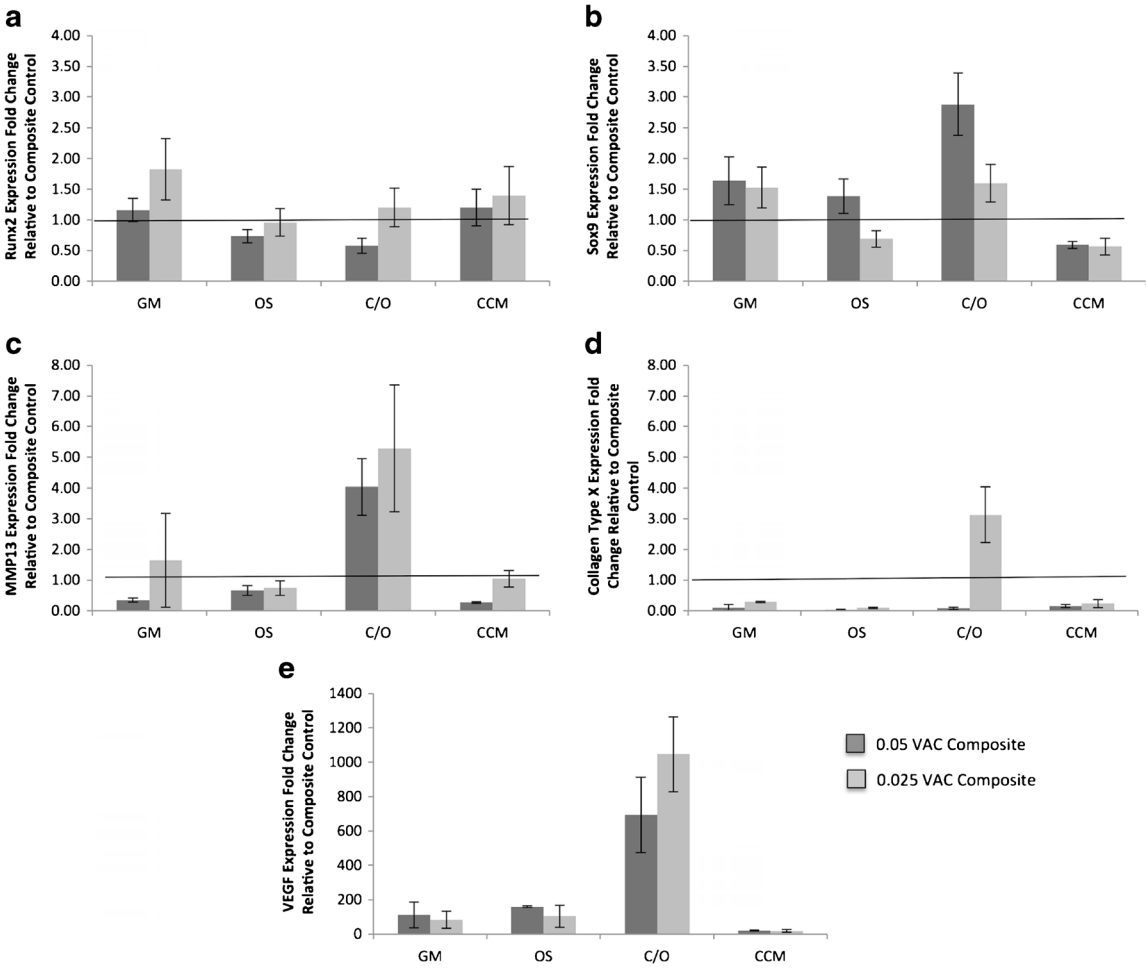

Fig. 8. Gene expression at day 28 for **a** Runx2, **b** Sox9, **c** MMP-13, **d** collagen type X, and **e** VEGF fold change relative to the composite control. Greater than 1.5-fold increase in upregulation is considered significant. $n = 3$ per group, values are mean ± SD

composites with a 10- to 1000-fold increase, and VEGF, as indicated by immunostaining, was incorporated in the ECM matrix for cells cultured on VAC composites. The upregulation of VEGF was the highest in C/O media conditions for cells on VAC composites at the 28-day time point, and VEGF production was also observed for cells cultured on the composite control in C/O media conditions. Angiogenesis is one of the most critical factors for successful bone formation throughout the scaffold and scaffold integration to the host tissue (63–65). Osteocalcin gene expression was low for all groups (data not shown), which was also shown by Patlolla and Arinzeh (46) for the composite control. However, the osteocalcin protein production was high for the VAC composites in C/O and CCM media. Studies show that insulin and insulin mimetics can increase osteocalcin protein production (2,17,18,88).

CONCLUSIONS

In this study, a bioactive composite scaffold containing VAC promoted osteogenic differentiation and supported cell growth. The novel VAC-containing composite also was able to stimulate VEGF gene expression and production, indicating its potential to induce angiogenesis *in vivo*. Cells on VAC composites demonstrated increased matrix formation and production of bone markers, ALP, and osteocalcin and upregulation of collagen type X and MMP-13 hypertrophic chondrocyte markers indicating the potential for this scaffold to support endochondral ossification. Establishing a model to assess endochondral bone formation *in vitro* might be of further interest when designing and evaluating scaffolds for bone tissue engineering.

ACKNOWLEDGMENTS

The authors would like to thank the support from the Coulter Foundation.

REFERENCES

1. Hu Y-C. Bone and cartilage tissue engineering. Gene therapy for cartilage and bone tissue engineering. SpringerBriefs in bioengineering. Berlin: Springer; 2014. p. 1–15.
2. Vanadium: the versatile metal: American Chemical Society; 2007. 502 p.
3. Kokubo T. Bioactive glass ceramics: properties and applications. Biomaterials. 1991;12(2):155–63.

4. Jones JR, Lin S, Yue S, Lee PD, Hanna JV, Smith ME, *et al*. Bioactive glass scaffolds for bone regeneration and their hierarchical characterisation. Proc Inst Mech Eng H J Eng Med. 2010;224(12):1373–87.
5. Rezwan K, Chen QZ, Blaker JJ, Boccaccini AR. Biodegradable and bioactive porous polymer/inorganic composite scaffolds for bone tissue engineering. Biomaterials. 2006;27(18):3413–31.
6. Arinzeh TL, Peter SJ, Archambault MP, Van Den Bos C, Gordon S, Kraus K, *et al*. Allogeneic mesenchymal stem cells regenerate bone in a critical-sized canine segmental defect. J Bone Joint Surg Am. 2003;85(10):1927–35.
7. Vo TN, Kasper FK, Mikos AG. Strategies for controlled delivery of growth factors and cells for bone regeneration. Adv Drug Deliv Rev. 2012;64(12):1292–309.
8. Habraken WJEM, Wolke JGC, Jansen JA. Ceramic composites as matrices and scaffolds for drug delivery in tissue engineering. Adv Drug Deliv Rev. 2007;59:234–48.
9. Blackwood KA, Bock N, Dargaville TR, Ann Woodruff M. Scaffolds for growth factor delivery as applied to bone tissue engineering. 2012. 25 p.
10. Shehzad S. The potential effect of vanadium compounds on glucose-6-phosphatase. Biosci Horiz. 2013;6.
11. Ji W, Sun Y, Yang F, van den Beucken JJJP, Fan M, Chen Z, *et al*. Bioactive electrospun scaffolds delivering growth factors and genes for tissue engineering applications. Pharm Res. 2011;28(6):1259–72.
12. Bose S, Tarafder S. Calcium phosphate ceramic systems in growth factor and drug delivery for bone tissue engineering: a review. Acta Biomater. 2012;8:1401–21.
13. Nie H, Wang C-H. Fabrication and characterization of PLGA/HAp composite scaffolds for delivery of BMP-2 plasmid DNA. J Controlled Release Off J Controlled Release Soc. 2007;120:111–21.
14. Sahoo S, Ang LT, Goh JC-H, Toh S-L. Growth factor delivery through electrospun nanofibers in scaffolds for tissue engineering applications. J Biomed Mater Res A. 2010;93A(4):1539–50.
15. Whitaker MJ, Quirk RA, Howdle SM, Shakesheff KM. Growth factor release from tissue engineering scaffolds. J Pharm Pharmacol. 2001;53(11):1427–37.
16. Srivastava AK, Mehdi MZ. Insulino-mimetic and anti-diabetic effects of vanadium compounds. Diabet Med. 2005;22(1):2–13.
17. Barrio DA, Cattáneo ER, Apezteguía MC, Etcheverry SB. Vanadyl(IV) complexes with saccharides. Bioactivity in osteoblast-like cells in culture. Can J Physiol Pharmacol. 2006;84(7):765–75. This paper is one of a selection of papers published in this special issue, entitled Second Messengers and Phosphoproteins—12th International conference
18. Barrio DA, Etcheverry SB. Vanadium and bone development: putative signaling pathways. Can J Physiol Pharmacol. 2006;84(7):677–86.
19. Barrio DA, Etcheverry SB. Potential use of vanadium compounds in therapeutics. Curr Med Chem. 2010;17(31):3632–42.
20. Paglia DN, Wey A, Hreha J, Park AG, Cunningham C, Uko L, *et al*. Local vanadium release from a calcium sulfate carrier accelerates fracture healing. J Orthop Res. 2014;32(5):727–34.
21. Paglia DN, Wey A, Park AG, Breitbart EA, Mehta SK, Bogden JD, *et al*. The effects of local vanadium treatment on angiogenesis and chondrogenesis during fracture healing. J Orthop Res. 2012;30(12):1971–8.
22. Zhang W, Shen X, Wan C, Zhao Q, Zhang L, Zhou Q, *et al*. Effects of insulin and insulin-like growth factor 1 on osteoblast proliferation and differentiation: differential signalling via Akt and ERK. Cell Biochem Funct. 2012;30(4):297–302.
23. Fulzele K, Clemens TL. Novel functions for insulin in bone. Bone. 2012;50(2):452–6.
24. Fukumoto S, Martin TJ. Bone as an endocrine organ. Trend Endocrinol Metab. 2009;20(5):230–6.
25. Williams A, Gillis A, McKenzie C, Po B, Sharma L, Micheli L, *et al*. Glycosaminoglycan distribution in cartilage as determined by delayed gadolinium-enhanced MRI of cartilage (dGEMRIC): potential clinical applications. Am J Roentgenol. 2004;182(1):167–72.
26. Zee T, Settembre C, Levine RL, Karsenty G. T-cell protein tyrosine phosphatase regulates bone resorption and whole-body insulin sensitivity through its expression in osteoblasts. Mol Cell Biol. 2012;32(6):1080–8.
27. Ferron M, Wei J, Yoshizawa T, Fattore AD, DePinho RA, Teti A, *et al*. Insulin signaling in osteoblasts integrates bone remodeling and energy metabolism. Cell. 2010;142(2):296–308.
28. Guo S. Insulin signaling, resistance, and the metabolic syndrome: insights from mouse models to disease mechanisms. J Endocrinol. 2014;220(2):T1–T23.
29. Koerner JD, Yalamanchili P, Munoz W, Uko L, Chaudhary SB, Lin SS, *et al*. The effects of local insulin application to lumbar spinal fusions in a rat model. Spine J. 2013;13(1):22–31.
30. Park AG, Paglia DN, Al-Zube L, Hreha J, Vaidya S, Breitbart E, *et al*. Local insulin therapy affects fracture healing in a rat model. J Orthop Res. 2013;31(5):776–82.
31. Paglia DN, Wey A, Breitbart EA, Faiwiszewski J, Mehta SK, Al-Zube L, *et al*. Effects of local insulin delivery on subperiosteal angiogenesis and mineralized tissue formation during fracture healing. J Orthop Res. 2013;31(5):783–91.
32. Schmid AC, Byrne RD, Vilar R, Woscholski R. Bisperoxovanadium compounds are potent PTEN inhibitors. FEBS Lett. 2004;566(1–3):35–8.
33. Mak LH, Vilar R, Woscholski R. Characterisation of the PTEN inhibitor VO-OHpic. J Chem Biol. 2010;3(4):157–63.
34. Lee NK, Sowa H, Hinoi E, Ferron M, Ahn JD, Confavreux C, *et al*. Endocrine regulation of energy metabolism by the skeleton. Cell. 2007;130(3):456–69.
35. Patti A, Gennari L, Merlotti D, Dotta F, Nuti R. Endocrine actions of osteocalcin. Int J Endocrinol. 2013;2013:846480.
36. Rodan GA. Bone homeostasis. Proc Natl Acad Sci U S A. 1998;95(23):13361–2.
37. Freeman FE, McNamara L. Endochondral priming: a developmental engineering strategy for bone tissue regeneration. Tissue Eng B Rev. 2016.
38. Freeman FE, Stevens HY, Owens P, Guldberg RE, McNamara LM. Osteogenic differentiation of mesenchymal stem cells by mimicking the cellular niche of the endochondral template. Tissue Eng Part A. 2016;22(19–20):1176–90.
39. Farrell E, Both SK, Odörfer KI, Koevoet W, Kops N, O'Brien FJ, *et al*. In-vivo generation of bone via endochondral ossification by in-vitro chondrogenic priming of adult human and rat mesenchymal stem cells. BMC Musculoskelet Disord. 2011;12:31.
40. Farrell E, van der Jagt OP, Koevoet W, Kops N, Van Manen CJ, Hellingman CA, *et al*. Chondrogenic priming of human bone marrow stromal cells: a better route to bone repair? Tissue Eng Part C Methods. 2008;15(2):285–95.
41. Bahney CS, Hu DP, Taylor AJ, Ferro F, Britz HM, Hallgrimsson B, *et al*. Stem cell-derived endochondral cartilage stimulates bone healing by tissue transformation. J Bone Miner Res. 2014;29(5):1269–82.
42. Yang W, Both SK, van Osch G, Wang Y, Jansen J, Yang F. Performance of different three-dimensional scaffolds for in vivo endochondral bone generation. Bone regeneration: from intramembranous to endochondral pathway. 2014:81.
43. Dennis SC, Berkland CJ, Bonewald LF, Detamore MS. Endochondral ossification for enhancing bone regeneration: converging native extracellular matrix biomaterials and developmental engineering in vivo. Tissue Eng Part B Rev. 2014;21(3):247–66.
44. Yang W, Both SK, van Osch GJVM, Wang Y, Jansen JA, Yang F. Effects of in vitro chondrogenic priming time of bone-marrow-derived mesenchymal stromal cells on in vivo endochondral bone formation. Acta Biomater. 2015;13:254–65.
45. Yang W, Yang F, Wang Y, Both SK, Jansen JA. In vivo bone generation via the endochondral pathway on three-dimensional electrospun fibers. Acta Biomater. 2013;9(1):4505–12.
46. Patlolla A, Arinzeh TL. Evaluating apatite formation and osteogenic activity of electrospun composites for bone tissue engineering. Biotechnol Bioeng. 2014;111(5):1000–17.
47. Shanmugasundaram S, Chaudhry H, Arinzeh TL. Microscale versus nanoscale scaffold architecture for mesenchymal stem cell chondrogenesis. Tissue Eng Part A. 2010;17(5–6):831–40.
48. Patlolla A, Collins G, Livingston Arinzeh T. Solvent-dependent properties of electrospun fibrous composites for bone tissue regeneration. Acta Biomater. 2010;6(1):90–101.

49. Briggs T, Matos J, Collins G, Arinzeh TL. Evaluating protein incorporation and release in electrospun composite scaffolds for bone tissue engineering applications. J Biomed Mater Res A. 2015;103(10):3117–27.
50. Deans RJ, Moseley AB. Mesenchymal stem cells: biology and potential clinical uses. Exp Hematol. 2000;28(8):875–84.
51. van der Kraan PM, van den Berg WB. Chondrocyte hypertrophy and osteoarthritis: role in initiation and progression of cartilage degeneration? Osteoarthr Cartil. 2012;20(3):223–32.
52. Miao D, Scutt A. Histochemical localization of alkaline phosphatase activity in decalcified bone and cartilage. J Histochem Cytochem. 2002;50(3):333–40.
53. Giuliani N, Lisignoli G, Magnani M, Racano C, Bolzoni M, Dalla Palma B, *et al*. New insights into osteogenic and chondrogenic differentiation of human bone marrow mesenchymal stem cells and their potential clinical applications for bone regeneration in pediatric orthopaedics. 2013. 11 p.
54. Quintana L, Zur Nieden NI, Semino CE. Morphogenetic and regulatory mechanisms during developmental chondrogenesis: new paradigms for cartilage tissue engineering. Tissue Eng Part B Rev. 2008;15(1):29–41.
55. Kawakami Y, Tsuda M, Takahashi S, Taniguchi N, Esteban CR, Zemmyo M, *et al*. Transcriptional coactivator PGC-1α regulates chondrogenesis via association with Sox9. Proc Natl Acad Sci U S A. 2005;102(7):2414–9.
56. Akiyama H. Control of chondrogenesis by the transcription factor Sox9. Mod Rheumatol. 2008;18(3):213–9.
57. Kolf CM, Cho E, Tuan RS. Mesenchymal stromal cells: biology of adult mesenchymal stem cells: regulation of niche, self-renewal and differentiation. Arthritis Res Ther. 2007;9(1):204.
58. Chen Q, Shou P, Zheng C, Jiang M, Cao G, Yang Q, *et al*. Fate decision of mesenchymal stem cells: adipocytes or osteoblasts [quest]. Cell Death Differ. 2016;23(7):1128–39.
59. Mendez-Ferrer S, Michurina TV, Ferraro F, Mazloom AR, MacArthur BD, Lira SA, *et al*. Mesenchymal and haematopoietic stem cells form a unique bone marrow niche. Nature. 2010;466(7308):829–34.
60. Inada M, Wang Y, Byrne MH, Rahman MU, Miyaura C, López-Otín C, *et al*. Critical roles for collagenase-3 (Mmp13) in development of growth plate cartilage and in endochondral ossification. Proc Natl Acad Sci U S A. 2004;101(49):17192–7.
61. Hartmann C. A Wnt canon orchestrating osteoblastogenesis. Trends Cell Biol. 2006;16(3):151–8.
62. D'Angelo M, Yan Z, Nooreyazdan M, Pacifici M, Sarment DS, Billings PC, *et al*. MMP-13 is induced during chondrocyte hypertrophy. J Cell Biochem. 2000;77(4):678–93.
63. Gerber H-P, Vu TH, Ryan AM, Kowalski J, Werb Z, Ferrara N. VEGF couples hypertrophic cartilage remodeling, ossification and angiogenesis during endochondral bone formation. Nat Med. 1999;5(6):623–8.
64. Dai J, Rabie ABM. VEGF: an essential mediator of both angiogenesis and endochondral ossification. J Dent Res. 2007;86(10):937–50.
65. Yang Y-Q, Tan Y-Y, Wong R, Wenden A, Zhang L-K, Rabie ABM. The role of vascular endothelial growth factor in ossification. In J Oral Sci. 2012;4(2):64–8.
66. Livak KJ, Schmittgen TD. Analysis of relative Gene expression data using real-time quantitative PCR and the $2^{-\Delta\Delta CT}$ method. Methods. 2001;25(4):402–8.
67. Ji W, Yang F, Seyednejad H, Chen Z, Hennink WE, Anderson JM, *et al*. Biocompatibility and degradation characteristics of PLGA-based electrospun nanofibrous scaffolds with nanoapatite incorporation. Biomaterials. 2012;33(28):6604–14.
68. Bose S, Roy M, Bandyopadhyay A. Recent advances in bone tissue engineering scaffolds. Trends Biotechnol. 2012;30(10):546–54.
69. Blackwood KA, Bock N, Dargaville TR, Ann Woodruff M. Scaffolds for growth factor delivery as applied to bone tissue engineering. Int J Polymer Sci. 2012;2012:174942.
70. Armentano I, Dottori M, Fortunati E, Mattioli S, Kenny JM. Biodegradable polymer matrix nanocomposites for tissue engineering: a review. Polym Degrad Stab. 2010;95(11):2126–46.
71. Srouji S, Ben-David D, Lotan R, Livne E, Avrahami R, Zussman E. Slow-release human recombinant bone morphogenetic protein-2 embedded within electrospun scaffolds for regeneration of bone defect: in vitro and in vivo evaluation. Tissue Eng Part A. 2010;17(3–4):269–77.
72. Nauth A, Ristevski B, Li R, Schemitsch EH. Growth factors and bone regeneration: how much bone can we expect? Injury. 2011;42:574–9.
73. Mouriño V, Cattalini JP, Boccaccini AR. Metallic ions as therapeutic agents in tissue engineering scaffolds: an overview of their biological applications and strategies for new developments. J R Soc Interface. 2012;9(68):401–19.
74. Martins A, Duarte ARC, Faria S, Marques AP, Reis RL, Neves NM. Osteogenic induction of hBMSCs by electrospun scaffolds with dexamethasone release functionality. Biomaterials. 2010;31(22):5875–85.
75. Ingavle GC, Leach JK. Advancements in electrospinning of polymeric nanofibrous scaffolds for tissue engineering. Tissue Eng Part B Rev. 2013;20(4):277–93.
76. Etcheverry SB, Crans DC, Keramidas AD, Cortizo AM. Insulin-mimetic action of vanadium compounds on osteoblast-like cells in culture. Arch Biochem Biophys. 1997;338(1):7–14.
77. Cortizo AM, Bruzzone L, Molinuevo S, Etcheverry SB. A possible role of oxidative stress in the vanadium-induced cytotoxicity in the MC3T3E1 osteoblast and UMR106 osteosarcoma cell lines. Toxicology. 2000;147(2):89–99.
78. Etcheverry SB, Barrio DA, Cortizo AM, Williams PAM. Three new vanadyl(IV) complexes with non-steroidal anti-inflammatory drugs (ibuprofen, naproxen and tolmetin). Bioactivity on osteoblast-like cells in culture. J Inorg Biochem. 2002;88(1):94–100.
79. Cortizo AM, Molinuevo MS, Barrio DA, Bruzzone L. Osteogenic activity of vanadyl(IV)–ascorbate complex: evaluation of its mechanism of action. Int J Biochem Cell Biol. 2006;38(7):1171–80.
80. Molinuevo M, Barrio D, Cortizo A, Etcheverry S. Antitumoral properties of two new vanadyl(IV) complexes in osteoblasts in culture: role of apoptosis and oxidative stress. Cancer Chemother Pharmacol. 2004;53(2):163–72.
81. Tchetina EV. Developmental mechanisms in articular cartilage degradation in osteoarthritis. Arthritis. 2011;2011:683970.
82. Xu Y, Pritzker K, Cruz T. Characterization of chondrocyte alkaline phosphatase as a potential mediator in the dissolution of calcium pyrophosphate dihydrate crystals. J Rheumatol. 1994;21(5):912–9.
83. Mueller MB, Tuan RS. Functional characterization of hypertrophy in chondrogenesis of human mesenchymal stem cells. Arthritis Rheum. 2008;58(5):1377–88.
84. Lian JB, McKee MD, Todd AM, Gerstenfeld LC. Induction of bone-related proteins, osteocalcin and osteopontin, and their matrix ultrastructural localization with development of chondrocyte hypertrophy in vitro. J Cell Biochem. 1993;52(2):206–19.
85. Fossett E, Khan WS, Longo UG, Smitham PJ. Effect of age and gender on cell proliferation and cell surface characterization of synovial fat pad derived mesenchymal stem cells. J Orthop Res. 2012;30(7):1013–8.
86. Jiang M, Wang X, Liu H, Zhou L, Jiang T, Zhou H, *et al*. Bone formation in adipose-derived stem cells isolated from elderly patients with osteoporosis: a preliminary study. Cell Biol Int. 2014;38(1):97–105.
87. Hattori T, Müller C, Gebhard S, Bauer E, Pausch F, Schlund B, *et al*. SOX9 is a major negative regulator of cartilage vascularization, bone marrow formation and endochondral ossification. Development. 2010;137(6):901–11.
88. Zoch ML, Clemens TL, Riddle RC. New insights into the biology of osteocalcin. Bone. 2016;82:42–9.